Genomic Priming of the Antisecretory Response to Estrogen in Rat Distal Colon throughout the Estrous Cycle

Fiona O'Mahony, Rodrigo Alzamora, Ho-Lam Chung, Warren Thomas, and Brian J. Harvey

Department of Molecular Medicine, Royal College of Surgeons in Ireland, Beaumont Hospital, Dublin 9, Ireland

The secretion of Cl^- across distal colonic crypt cells provides the driving force for the movement of fluid into the luminal space. 17β-Estradiol (E2) produces a rapid and sustained reduction in secretion in females, which is dependent on the novel protein kinase Cδ (PKCδ) isozyme and PKA isoform I targeting of KCNQ1 channels. This sexual dimorphism in the E2 response is associated with a higher expression level of PKCδ in female compared with the male tissue. The present study revealed the antisecretory response is regulated throughout the female reproductive (estrous) cycle and is primed by genomic regulation of the kinases. E2 (1–10 nM) decreased cAMP-dependent secretion in colonic epithelia during the estrus, metestrus, and diestrus stages. A weak inhibition of secretion was demonstrated in the proestrus stage. The expression levels of PKCδ and PKA fluctuated throughout the estrous cycle and correlated with the potency of the antisecretory effect of E2. The expression of PKCδ and PKA were up-regulated by estrogen at a transcriptional level via a PKCδ-MAPK-cAMP response element-binding protein-regulated pathway indicating a genomic priming of the antisecretory response. PKCδ was activated by the membrane-impermeant E2-BSA, and this response was inhibited by the estrogen receptor antagonist ICI 182,780. The 66-kDa estrogen receptor-α isoform was present at the plasma membrane of female colonic crypt cells with a lower abundance found in male colonic crypts. The study demonstrates estrogen regulation of intestinal secretion both at a rapid and transcriptional level, demonstrating an interdependent relationship between both nongenomic and genomic hormone responses. (***Molecular Endocrinology*** **23: 1885–1899, 2009)**

The absorption and secretion of salt and water is a major physiological role of the large intestine. Estrogen is known to be a salt-retaining steroid hormone in many tissues. Clinically, salt and water retention is observed during high estrogenic states (1). The synthetic derivative of estradiol, ethinylestradiol, which is found in oral contraceptives, hormone replacement therapy, and the morning after pill, has been demonstrated to cause retention of salt and water in the female body (2). For many years, it has been recognized that cyclical changes in the levels of ovarian hormone secretions effect whole-body water and electrolyte homeostasis (3, 4). The kidneys, lungs, and large intestine are the major regulators of whole-body water and salt balance. Previously, these organs were not recognized as being targeted by circulating sex steroids. It is now known that estrogen can influence Na^+ retention in all three tissues (5–7). Certain phases of the reproductive cycle have been implicated in influencing intestinal physiology in three ways: function, cell proliferation/profile, and electrolyte and fluid movement. In addition, differences in the colonic transit time of the feces between phases of the menstrual cycle have been documented and in particular a slowing in the luteal phase due to less fluid content (8, 9). The luteal phase of the menstrual cycle occurs after ovulation lasting from 10–16 d and is referred to as the window of implantation. The

ISSN Print 0888-8809 ISSN Online 1944-9917
Printed in U.S.A.

doi: 10.1210/me.2008-0248 Received July 22, 2008. Accepted August 18, 2009.
First Published Online October 21, 2009

Abbreviations: CRE, cAMP response element; CREB, CRE-binding protein; DAPI, 4′,6-diamidino-2-phenylindole; E2, 17β-estradiol; ERα, estrogen receptor-α; MEK, MAPK kinase; PKACI, protein kinase A catalytic subunit isoform I; PKCδ, protein kinase Cδ; qRT, quantitative real-time; WGA, wheat germ agglutinin.

estrogen peak occurs previous to the luteal phase during ovulation. The uterus continues to expand throughout this phase, which involves retention of bodily fluid (10) and fluid expansion in the endometrium (11). Given the impact that high-estrogen states has on whole-body fluid volume and uterine swelling, it is surprising so little is known of the molecular mechanisms for estrogen effects on fluid and electrolyte transport in the body and, in particular, the intestine. It is possible that the regulation of Cl^- secretion by estrogen in the distal colon and the components of the molecular mechanism involved may vary depending on the hormonal background of the female.

Cl^- secretion in the distal colon can be up-regulated by two distinct mechanisms: an increase in intracellular Ca^{2+} (12) or cAMP activity (13). Cl^- enters the cell across the basolateral membrane by cotransport with K^+ and Na^+. Cl^- is then secreted via CFTR channels at the apical membrane and other Cl^- channels. A basolateral K^+ conductance maintains the favorable negative membrane potential to drive Cl^- electrodiffusion into the lumen. The major K^+ channels providing the route for K^+ recycling are cAMP-dependent KCNQ1 channels and Ca^{2+}-activated KCNN4 channels. In human colonic tissue, it has been demonstrated that blocking basolateral K^+ activity decreases forskolin-induced Cl^- secretion (14). Similarly, pretreatment of colonic tissue with 17β-estradiol (E2) (0.1–100 nM) significantly reduced forskolin-stimulated Cl^- secretion (7). We have recently demonstrated that the E2 inhibition of secretion in rat distal colonic epithelia is female sex specific (15). The mechanism was shown to involve protein kinase Cδ (PKCδ) and PKA isoform I-dependent modulation of KCNQ1 channel activity.

The genomic action of estrogen involves binding of the hormone to the cytosolic estrogen receptor-α (ERα) followed by translocation of this complex to the nucleus whereupon it binds the estrogen response element inducing transcription. It is known that rapid actions of E2 may prime gene transcription via the activation of second messengers, which in turn target transcription factors. The cAMP response element (CRE)-binding protein (CREB) was found in many tissues to be phosphorylated in response to PKA and MAPK activation by estrogen (16). Activated CREB binds to the CRE found in the promoter region of many genes. The outcome of CREB activation and binding is an increase/decrease in the transcription of certain genes. Upon binding to the CRE, the CREB-binding protein is recruited and coactivates CREB. Binding of the CREB-binding protein to the CREB-DNA complex is enhanced by further binding of the steroid coactivator receptor 1 (SRC1) in the case of steroid receptor-dependent transcription (17). Steroid receptor-independent activation of this transcription factor occurs in response to a wide variety of extracellular signals such as growth hormones, steroid hormones, and neurotransmitters. Rapid CREB phosphorylation by estrogen independent of the classical receptor has previously been reported (18). Priming of the genomic response during the rapid nongenomic phase of action of steroid hormones and transcriptional regulation of the nongenomic responses are hot topics in endocrinology. Cross talk between the rapid nongenomic and genomic actions of estrogen occurring via membrane ERα, protein kinases, and modulation of the CREB transcription factor was investigated in this paper.

Results

The potency of E2 inhibition of cAMP-dependent Cl^- secretion in female rat colonic epithelia varies throughout the estrous cycle

We have previously demonstrated that E2 inhibits cAMP-dependent Cl^- secretion via a PKCδ/PKA signaling pathway (15). Basolateral addition of heat-stable enterotoxin (STa) (*E.Coli,* potent activator of cAMP-dependent secretion) (1 μg/ml) induced an instantaneous and sustained increase (100%) in short circuit current (I_{SC}). E2 (10 nM) reduced the STa effect on I_{SC} with maximal inhibition of secretion observed at estrus, metestrus, and diestrus (percent secretion: estrus, 57 ± 4%; metestrus, 60 ± 3%; diestrus, 57 ± 4%; n = 5; $P < 0.001$; Fig. 1A). The E2 effect on secretion at proestrus was insignificant and comparable to that of the male tissue (percent secretion: proestrus, 87 ± 5%; male, 101 ± 7%; Fig. 1A). Inhibition of secretion in proestrus became significant at supraphysiological levels of E2 (percent secretion: 100 nM E2, 70 ± 3%; n = 5; $P < 0.001$). No effects upon secretion were noted with the addition of the estrogen vehicle carrier MeOH (data not shown). These results demonstrate the antisecretory effect of E2 is estrous cycle dependent.

Estrous cycle differences in PKA activation in response to E2 in female rat distal colonic crypts

Isolated female rat distal colonic crypts from each stage of the cycle were exposed to E2 (10 nM) or equivalent vehicle (0.01%) for the duration of 2, 5, and 15 min. Total lysates were prepared and analyzed using the PepTag assay for the nonradioactive detection of cAMP-dependent protein. Differences were recorded as fold values of treated over control.

PKA was activated in female distal colonic crypts at the estrus stage in response to E2 at 5 min (2.8 ± 0.4-fold higher, n = 5; $P < 0.001$; Fig. 1B). In contrast, PKA was not activated at the proestrus stage in response to E2 (n =

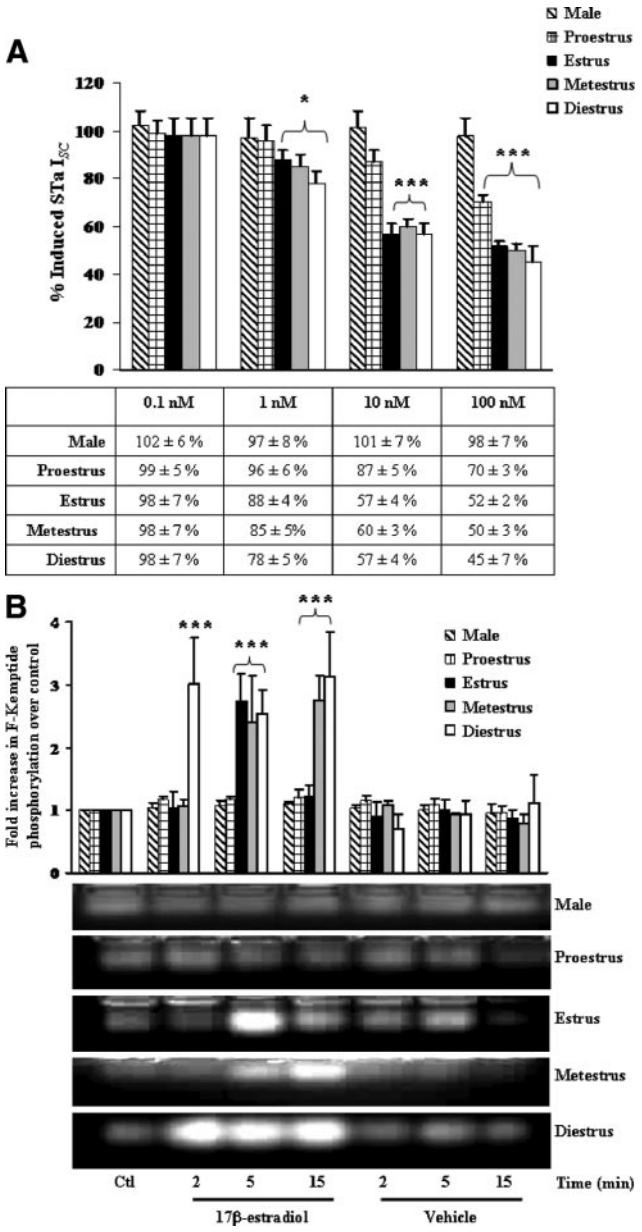

	0.1 nM	1 nM	10 nM	100 nM
Male	102 ± 6 %	97 ± 8 %	101 ± 7 %	98 ± 7 %
Proestrus	99 ± 5 %	96 ± 6 %	87 ± 5 %	70 ± 3 %
Estrus	98 ± 7 %	88 ± 4 %	57 ± 4 %	52 ± 2 %
Metestrus	98 ± 7 %	85 ± 5%	60 ± 3 %	50 ± 3 %
Diestrus	98 ± 7 %	78 ± 5 %	57 ± 4 %	45 ± 7 %

FIG. 1. Antisecretory effect of E2 on cAMP-induced Cl^- secretion is estrous cycle dependent and is primed by differential activation of PKA throughout the cycle. A, Representative recording of the effect of E2 (0.1–100 nM) on heat-stable enterotoxin (STa)-induced (1 μg/ml) short-circuit current (I_{SC}) in male and female rat colonic epithelia. The female tissue was obtained at each stage of the estrous cycle. Male tissue was used as a control in this paper because a previous report demonstrates a lack of inhibition (15). Colonic mucosas were treated with the secretory agent basolaterally, and E2 was added at the peak of the response. B, Representative image of PKA phosphorylation of an F-Kemptide PepTag in cellular extracts from female rat distal colonic crypts at each stage of the estrous cycle and male tissue in response to E2 (10 nM). CTL, Control. The graphs represent densitometric analysis at specific time points of E2 treatment. Values are given as fold changes in PKA phosphorylation of the F-Kemptide PepTag for all samples. Values are displayed as ± SEM (n = 5 for A; n = 4 for B). *, $P < 0.05$; ***, $P < 0.001$.

6; $P > 0.05$; Fig. 1B). The kinetics of PKA activation at metestrus (Fig. 1B) was similar to that of estrus. During diestrus, the activation of PKA was more rapid and sustained (15 min, 3.1 ± 0.7-fold higher, n = 3; $P < 0.001$; Fig. 1B). Thus, PKA activation in response to estrogen is dependent on the stage of the estrous cycle.

Estrous cycle dependence of PKA and PKCδ basal expression

Untreated cellular protein extracts of isolated rat distal colonic crypts at each stage of the estrous cycle were prepared, quantified, and subjected to Western blot analysis and probed using specific antibodies to endogenous levels of PKA catalytic subunit isoform I (PKACI) and PKCδ. The expression levels were normalized for loading differences by probing for β-actin. In all cases, the differences were expressed as densometric values (pixel intensity) for each stage of the estrous cycle.

Basal expression amounts of PKCδ increased throughout the reproductive cycle with a peak in expression at the diestrus stage (proestrus *vs.* diestrus, 5.1 ± 1.5-fold higher, n = 4; $P < 0.001$) (further exposure of autoradiographic film demonstrated expression in female proestrus, not shown) (Fig. 2A). Basal expression amounts of PKACI increased throughout the cycle, also with a peak in expression at the diestrus stage (proestrus *vs.* diestrus, 1.9 ± 0.2-fold higher, n = 3; $P < 0.01$; Fig. 2B). The estrous cycle changes in protein kinase expression after the E2 peak in proestrus indicate estrogenic genomic regulation of expression levels.

CREB is expressed in female distal colonic crypts, and the expression levels are regulated during the estrous cycle

To date, the expression of CREB has not been shown in the rat distal colonic epithelia and expression was confirmed by RT-PCR using gene-specific primers in both male and female tissues (data not shown).

A marked estrous cycle difference in basal protein expression was demonstrated. The expression of CREB was low (further exposure of autoradiographic film demonstrated expression in male and female proestrus, not shown) at the proestrus stage (proestrus *vs.* estrus, 2 ± 0.2-fold higher, n = 4; $P < 0.05$; Fig. 3). CREB expression was maximal at metestrus (estrus *vs.* metestrus, 2.6 ± 0.2-fold higher, n = 4; $P < 0.001$). CREB basal expression levels are regulated throughout the estrous cycle in rat distal colonic epithelia, indicating plasticity in the transcriptional capacity of the female colonic cells.

CREB is rapidly phosphorylated in response to E2

Colonic crypts at the estrus stage of the cycle were isolated from female rats and adhered to glass slides. Immunofluorescent staining was performed to stain for phospho-CREB (Ser133) followed by a 4′,6-diamidino-2-phenylindole (DAPI) counterstain. DAPI stains DNA and was used to track the phosphorylation events of

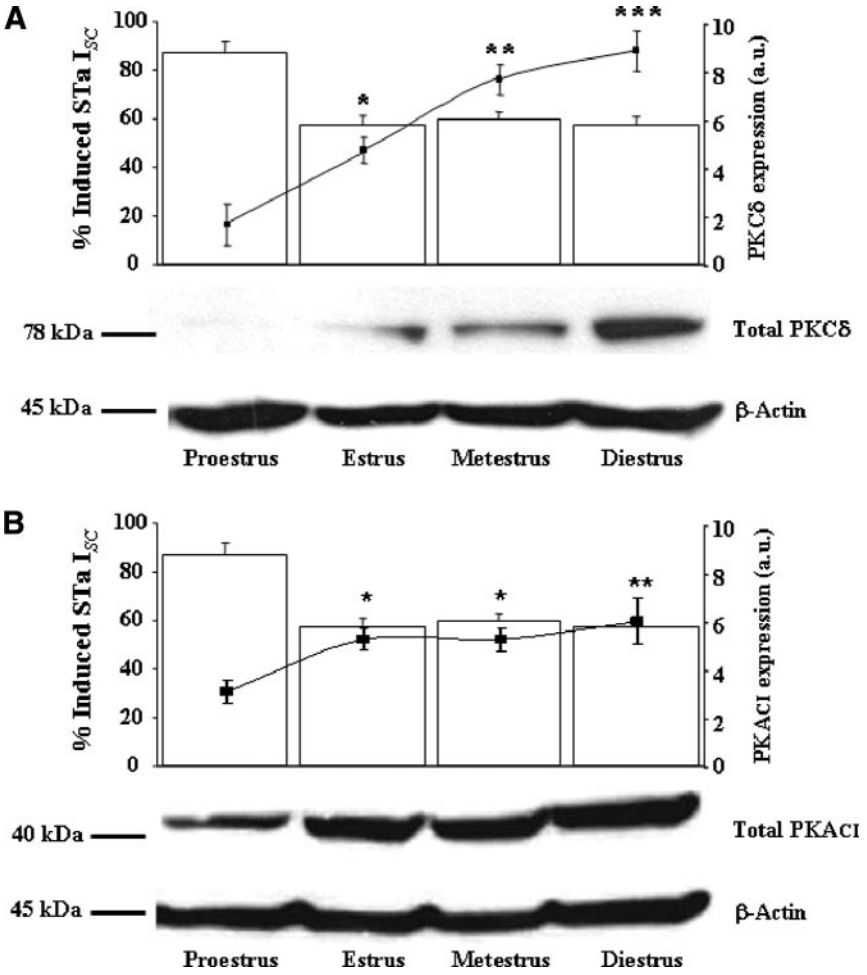

FIG. 2. The expression levels of PKCδ and PKACI increases throughout the estrous cycle after proestrus. The antisecretory effect of E2 (10 nM) is related to the expression levels of both kinases in the colonic tissue. A, Inhibitory effect of E2 on heat-stable enterotoxin (STa)-induced (1 μg/ml) Cl^- secretion in colonic mucosa at each stage of the estrous cycle (*bar graph*) compared with PKCδ protein levels (*line graph*). B, Inhibitory effect of E2 on heat-stable enterotoxin-induced (1 μg/ml) Cl^- secretion in colonic mucosa at each stage of the estrous cycle (*bar graph*) compared with PKACI protein levels (*line graph*).The figures show representative Western blots of the kinases. Values on the graphs are given as a mean fold increase compared with proestrus samples. Values are displayed as mean ± SEM (n = 4 for A; n = 3 for B). *, $P < 0.05$; **, $P < 0.01$; ***, $P < 0.001$. a.u., Arbitrary units; I_{SC}, short-circuit current.

CREB in the nucleus. After incubation with E2 for 2 min, the intensity of the phospho-CREB signal increased, indicating the induction of CREB phosphorylation (Fig. 4A). In colonic crypt cells, the nucleus resides close to the basolateral membrane. The CREB phosphorylation was located toward the basolateral side of the cells and when combined with the nuclear-specific DAPI stain, the merged image indicated early nuclear localization of phospho-CREB. The phosphorylation of CREB occurred throughout the pole of the crypt. The phosphorylation of CREB in the nuclei of crypt cells treated with E2 was detected within 2 min, and the proportion of nuclei with detectable phospho-CREB increased after 5 min (Fig. 4B). Before E2 treatment, the phospho-CREB signal was weak and diffuse around the DNA signal. These results demonstrate that estrogen promotes CREB phosphorylation within the vicinity of the DNA.

P44 MAPK is rapidly phosphorylated in response to E2 via a PKCδ-dependent pathway

P42 and P44 MAPK activity was assessed by measuring phosphorylation at Thr202/Tyr204 in the activation loop of the protein by Western blot analysis. An increase in activity was demonstrated for P44 MAPK at 2 and 5 min in response to E2 (10 nM) treatment (5 min, 4.1 ± 0.4-fold higher, n = 5, $P < 0.0001$; Fig. 5A). However, no increase in the activity of P42 MAPK was elicited in response to E2 (5 min, 1.7 ± 0.3, n = 5; $P > 0.05$; Fig. 5A). Similarly, E2 did not activate P38 MAPK (data not shown). It is known that P38 MAPK and P42 MAPK share a highly similar amino acid sequence (19). The differential activation of the P42 and P44 MAPK isoforms may increase the specificity of the signaling pathway. Both P42 and P44 share a common spatial distribution and upon activation translocate together to the nucleus (20). It has been demonstrated that these kinases may also work separately in some tissues and have independent functions (21).

Pretreatment of colonic crypts with the PKCδ-specific inhibitor rottlerin (10 μM) (22) blocked the estrogen activation of P44 MAPK activity (0.8 ± 0.1-fold higher, n = 3; $P > 0.05$; Fig. 5B). This result demonstrates the sequence of activation of PKCδ and P44 MAPK in female colonic crypts in response to E2. In addition to its function in the activation of the rapid antisecretory mechanism, PKCδ is also an essential signaling intermediate for activating P44 MAPK, a known regulator of transcription.

CREB phosphorylation in response to E2 is MAPK and PKA dependent

Colonic crypts were isolated at the estrus stage from female rats and adhered to glass slides. Immunofluorescent staining was performed for phospho-CREB (Ser133) followed by a DAPI counterstain. Again, after incubation with E2 (10 nM) for 5 min, the intensity of the phospho-CREB signal increased indicating phosphorylation of CREB

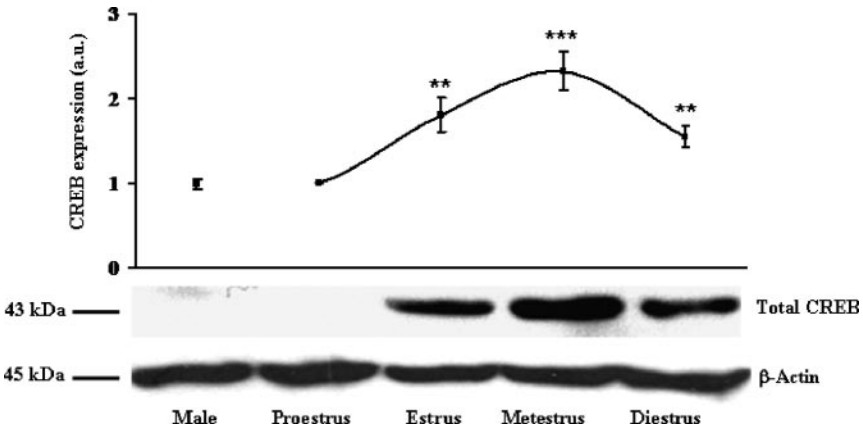

FIG. 3. The transcription factor CREB basal expression levels differ throughout the estrous cycle. CREB protein expression was analyzed throughout the estrous cycle. The figure shows a representative Western blot of the transcription factor. Values on the graphs are given as a mean fold increase compared with proestrus samples. Values are displayed as mean ± SEM (n = 3). **, $P < 0.01$; ***, $P < 0.001$.

(Fig. 6). Pretreatment with PD 98059 (25 μM), a MAPK kinase (MEK)-1 inhibitor (23), blocked the phosphorylation of CREB at Ser133. This result shows that the estrogen-induced phosphorylation of CREB occurs via a P44 MAPK-dependent pathway. PKA is a common regulator of CREB phosphorylation. We have previously shown that PKA is rapidly phosphorylated in response to E2 in a PKCδ-dependent manner in female colonic crypts. We investigated a possible involvement of PKA in the CREB transcriptional pathway. Pretreatment of colonic crypts with H89 (10 μm), a specific PKA inhibitor (24), blocked the phosphorylation of CREB at Ser133. The rapid CREB phosphorylation in response to E2 is P44 MAPK and PKA dependent.

Phosphorylated MAPK translocates to the nuclei in response to E2

To confirm the translocation of phospho-MAPK to the nucleus, colonic crypts were stained for phospho-MAPK and analyzed using confocal microscopy. Colonic crypts at the estrus stage of the cycle were isolated from female rats, adhered to glass slides, and subjected to immunofluorescent staining. After incubation with E2 for 2 and 5 min, the intensity of the phospho-MAPK signal increased, indicating the induction of MAPK phosphorylation (Fig. 7A). An increase in the level of phospho-MAPK was observed in the nucleus, demonstrating that phospho-MAPK rapidly translocates to the nucleus upon estrogen treatment. The P44 isoform was immunoprecipitated from estrogen-treated colonic crypts, and Western blot analysis was used to blot for associated CREB. P44 MAPK associated with the CREB transcription factor at 5 min, and the association was transient (1.8 ± 0.2-fold higher, n = 3; $P < 0.01$; blot *inset*, Fig. 7A).

PKACI translocates to the nucleus region in response to E2

To confirm the translocation of PKA to the nucleus, colonic crypts were stained for PKA and analyzed using confocal microscopy. Colonic crypts were isolated at the estrus stage of the cycle. After incubation with E2 for 2 min, the intensity of the PKA signal at the edge of the nuclear signal was increased (Fig. 7B). It was demonstrated to be inside the nucleus as the merged image (*yellow*) demonstrates the kinase to be within the vicinity of the DNA signal. This would allow PKA to also directly phosphorylate CREB in addition to MAPK. This dual regulation of CREB by both MAPK and PKA concurrently has previously been documented (25, 26), increasing the level of CREB phosphorylation. This translocation was blocked by the addition of the MEK-1 inhibitor PD 98059 indicating that MAPK recruits PKA in the regulation of CREB.

E2 increases the mRNA levels of PKCδ, PKA isoform I, and CREB via a MAPK/PKA pathway

In a previous study, it was demonstrated that chronic exposure to chronic E2 (10 nM) dramatically increased transcription of PKCδ mRNA in colonic crypts isolated from female rats (15). This response was absent in the male. In the present study, total RNA was extracted from female colonic crypts at estrus. Specific primers to PKCδ, PKACI, PKARI, CREB, and β-actin were synthesized (MWG-Biotech, London, UK). The PKA isoform I has previously been shown to be the isoform activated in the rapid estrogen signaling pathway in rat colonic tissue (15, 27). Expression differences in the protein kinase levels were demonstrated in this study, and we investigated whether mRNA expression was also regulated by estrogen.

E2 (10 nM) induced an up-regulation of mRNA levels for all the signaling components studied: PKCδ (5 ± 1.4-fold higher, n = 4; $P < 0.01$), PKACIα (6 ± 2-fold higher, n = 4; $P < 0.01$), and CREB (1.5 ± 0.06-fold higher, n = 4; $P < 0.05$) using quantitative real-time (qRT)-PCR analysis (Fig. 8, A, B, and D). No change in mRNA expression levels were observed for PKACIβ (1 ± 0.005-fold higher, n = 4; $P > 0.05$), indicating that E2 specifically regulates the PKACIα subtype in female rat distal colon. The up-regulation of PKCδ, PKACIα, and CREB was blocked by pretreatment with PKA and MAPK inhibitors. The inhibitory data support the involvement

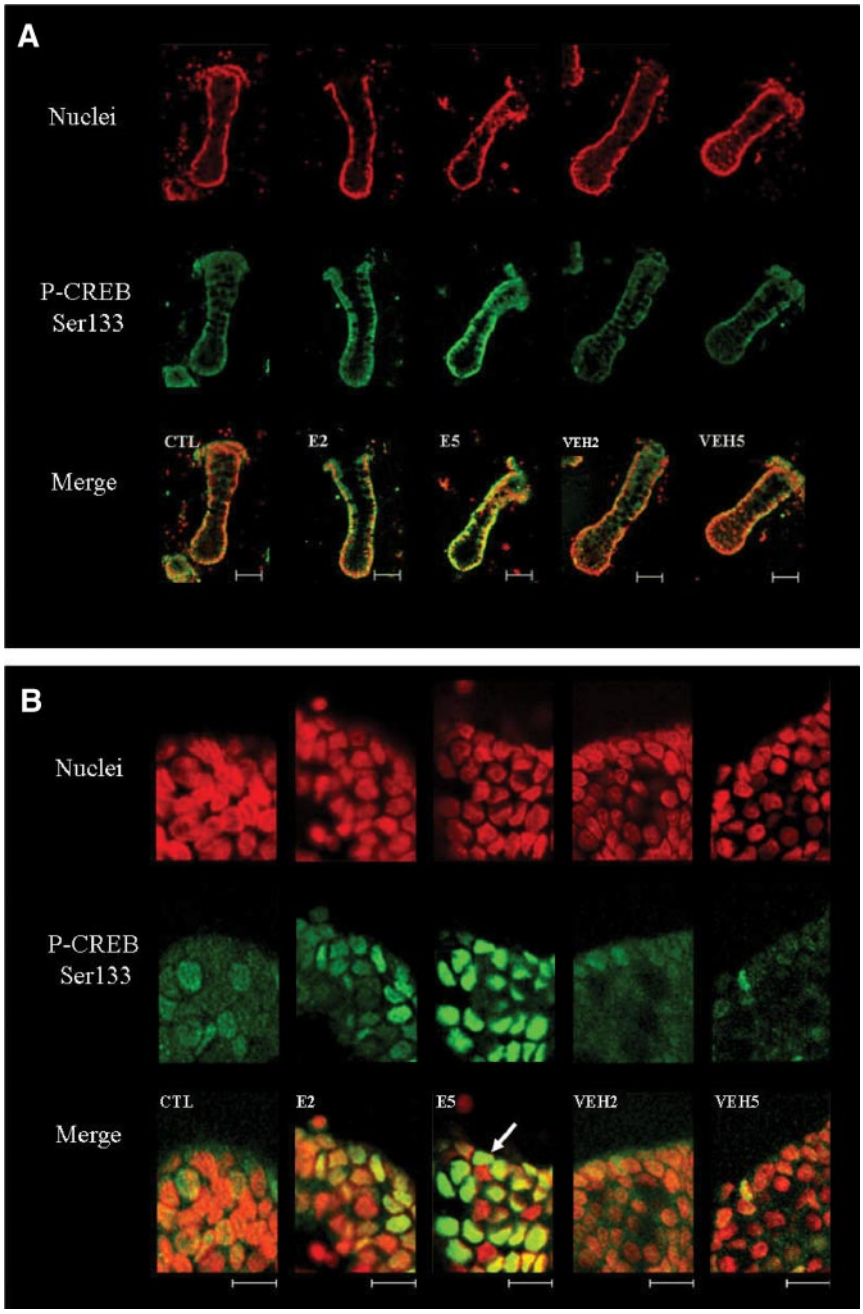

FIG. 4. E2 (10 nM) rapidly induces phosphorylation of CREB in female rat colonic crypts isolated at the estrus stage. A, Isolated colonic crypts were adhered to glass slides, treated as required, and fixed in 4% paraformaldehyde followed by permeabilization in 0.2% Triton X-100 in 1× PBS. Phospho-CREB (P-CREB) was stained using an antibody to Ser133. The slides were mounted using VectaShield media containing the DNA stain DAPI. A single (xy) plane through the colonic crypt structure is shown using an ×40 oil objective. B, Further magnification using a ×63 oil objective was carried out. Nuclei at the base (*bottom*) of the crypt were imaged again using a single (xy) plane through the colonic crypt. *Red* shows the nuclei staining, and the *green* shows the phospho-CREB staining. The merged *yellow* images indicate that CREB was phosphorylated in the vicinity of the DNA. *Arrow* indicates an area of CREB phosphorylation. CTL, Control; E2, E2 for 2 min; E5, E2 for 5 min; VEH2, vehicle for 2 min; VEH5, vehicle for 5 min. Each treatment was examined in three rats with five to seven crypts for each treatment per rat. Phosphorylation of CREB in the nuclei of vehicle-treated cells did not increase above basal levels. *Scale bar*, 20 μm (A) and 5 μm (B).

for the CREB transcription factor in driving the expression of the signaling kinases at an RNA level. At present, there is no significant inhibitor of the CREB transcription factor.

E2-induced rapid kinase signaling and transcriptional responses are transduced via a membrane-associated ERα

We investigated whether the phosphorylation of PKCδ in response to E2 occurred via a membrane-bound ERα protein. We have previously reported the phosphorylation of PKCδ at Ser643 in response to E2 (15). The impeded ligand form of estrogen E2-BSA (10 nM) induced rapid (5 min) phosphorylation of PKCδ (4 $\pm$ 0.3-fold higher, n = 3; $P < 0.001$) (Fig. 9A). The membrane-impermeant E2-BSA (10 nM) stimulated PKCδ phosphorylation comparable to unconjugated E2. The phosphorylation of PKCδ was inhibited by pretreatment with the ER inhibitors ICI 182,780 (1 μM) and tamoxifen (10 μM). To determine whether the transcriptional responses of E2 were via a membrane ER, we investigated whether E2-BSA-induced up-regulation of PKCδ mRNA. E2-BSA both at 5 and 10 nM induced an increase in the level of PKCδ mRNA, indicating regulation via a membrane ER (5 nM E2, 1.6 $\pm$ 0.3-fold higher; 10 nM E2, 2.2 $\pm$ 0.2-fold higher; n = 2; Fig. 9B). Male and female colonic crypt samples were fractionated, and the plasma membrane was extracted. The quality of the plasma membrane fraction was checked by immunoblotting using the Na^+K^+ ATPase as a marker (Fig. 9C). The level of detectable ERα 66-kDa protein at the plasma membrane was low in the male compared with the female fraction where the protein was present at a level comparable to that of a whole-cell lysate preparation of MCF-7 cells (Fig. 9C). The truncated 46-kDa version of ERα was not present in plasma membrane fractions of colonic crypts from males or females (Fig. 9C). Whole-cell lysate analysis showed a very low level of 46-kDa ERα (data not shown). Isolated female colonic crypts at the estrus stage were subjected to immunofluorescence and confocal analysis to determine location of the receptor and further confirm that ERα is membrane bound in distal colonic

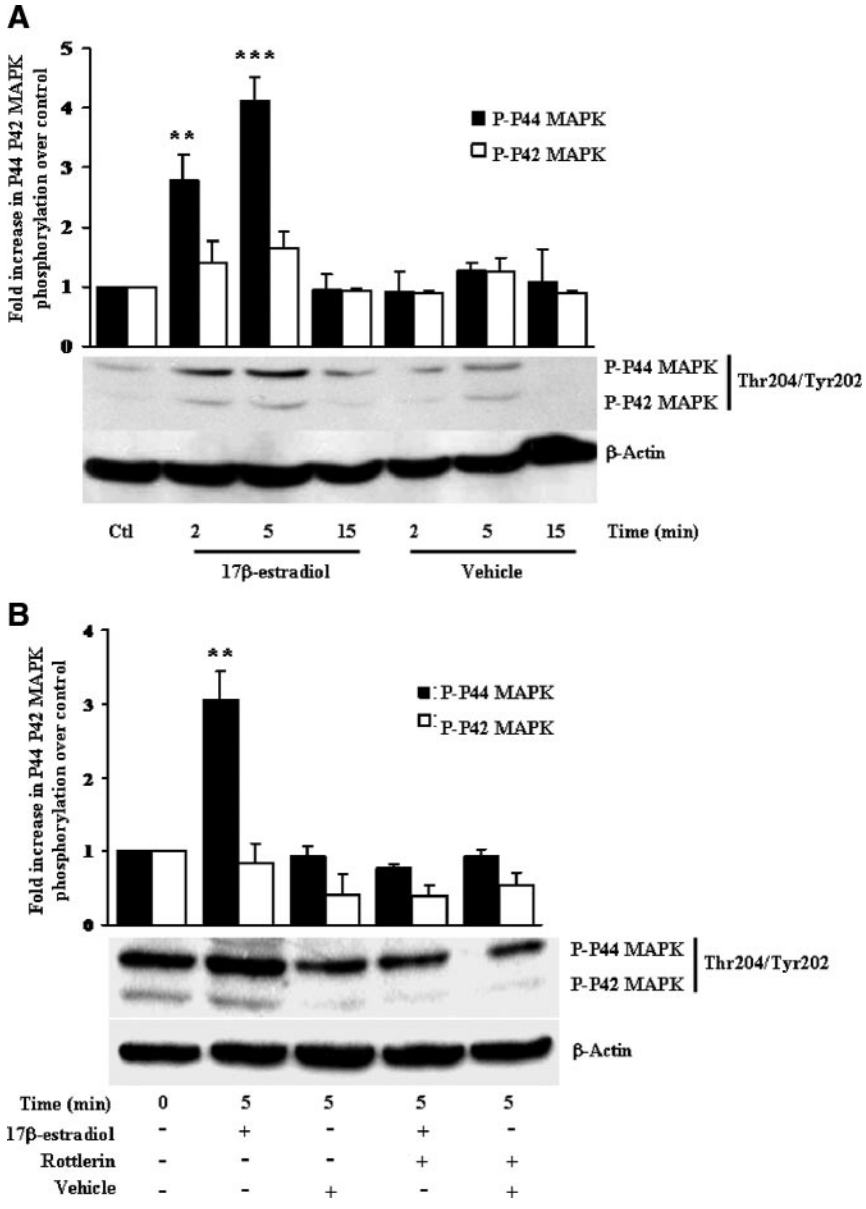

FIG. 5. P44 MAPK is rapidly activated in response to E2 (10 nM) in female rat distal colonic crypts and is PKCδ dependent. A, Representative blot of P44 MAPK phosphorylation levels at Thr202/Tyr204 in cellular extracts from female rat distal colonic crypts at the estrous cycle. P-P42, Phospho-P42; P-P44, phospho-P42. B, Rottlerin (10 μM) prevented the activation of P44 MAPK activation at 5 min. The graphs represent densitometric analysis at specific time points of E2 treatment. CTL, Control. Values are given as fold changes in P44/P42 MAPK phosphorylation (activity) for colonic crypt samples. Values are displayed as mean ± SEM (n = 3 for A and B). **, $P < 0.01$; ***, $P < 0.001$.

crypts. Wheat germ agglutinin (WGA) was used to stain for plasma membrane, and ERα association at the basolateral membrane was investigated. ERα was detected and localized at the basolateral plasma membrane. Association of the receptor with the plasma membrane is apparent from the merged image of plasma membrane and ERα (Fig. 9D). This is the first report of a membrane-associated full-length ERα in the distal colon. Figure 9E demonstrates estrous cycle differences in 66-kDa ERα in whole-cell lysates from female colonic crypts.

Discussion

E2 induces an antisecretory response in the female rat distal colon (15). The antisecretory action of E2 is estrous cycle dependent, indicating the response is differentially primed depending on the level of sex steroids in the blood plasma. Reproductive cycle regulation of cross-organ interactions has been reported between the reproductive, gastrointestinal, and urinary tracts. A previous study has shown a level of functional communication between the uterus, colon, and bladder (28). In another study, inflammation of the colon has been demonstrated to affect uterine contractility and in turn inflammation is also affected by the estrous cycle (29).

The endometrial implantation window is associated with expansion of the extracellular fluid volume. Here we show that the fluctuating hormone levels throughout the estrous cycle are correlated with changes in the potential for estrogen to inhibit secretion in the colon.

We have previously described the molecular mechanism of estrogen inhibition of Cl^- secretion in the female distal colon (15). The antisecretory mechanism involves the rapid and transient up-regulation of PKCδ/PKA activity. It was demonstrated that PKCδ phosphorylates PKA, which in turn associates with the KCNQ1 channel inducing serine phosphorylation of the channel. Phosphorylation of the KCNQ1 channel results in a decrease in basolateral K^+ recycling, which reduces the electrical driving force for Cl^- secretion. The key signaling factor underlying the sexual dimorphism in E2 action is the differential regulation of PKCδ at a transcriptional level. PKCδ expression was higher in the female compared with the male. The present study identified key estrous cycle-dependent changes in the expression of PKCδ and PKA both at transcript and protein levels.

There are few reports in the literature on estradiol regulation of kinase expression throughout the reproductive cycle. Estrogen has previously been shown to regulate

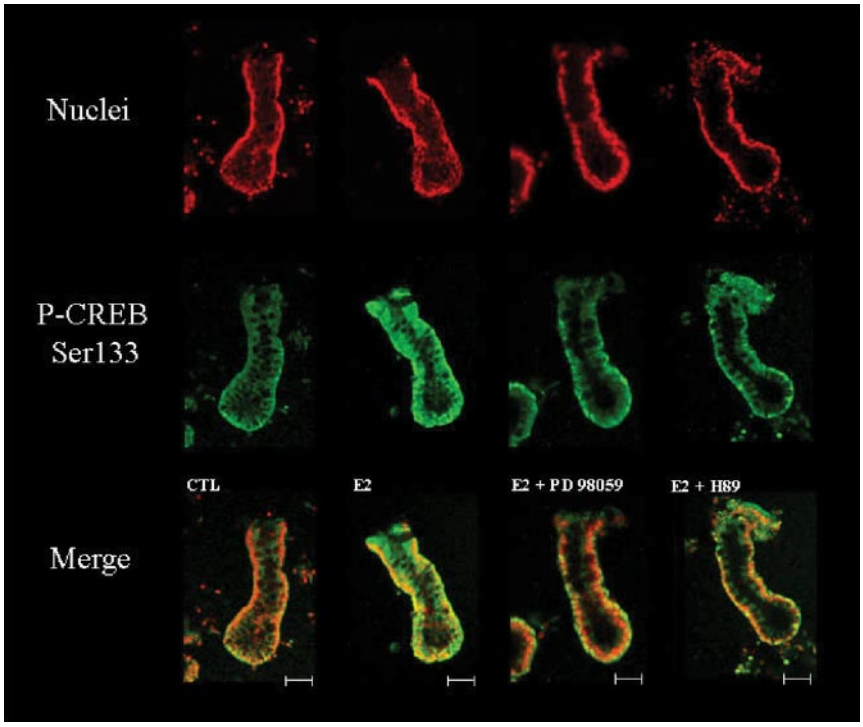

FIG. 6. Rapid E2-induced phosphorylation of CREB in female rat colonic crypts is via a MAPK/PKA-dependent pathway. Isolated colonic crypts were adhered to glass slides, treated as required, and fixed in 4% paraformaldehyde followed by permeabilization in 0.2% Triton X-100 in 1× PBS. Phospho-CREB (P-CREB) was stained using an antibody to Ser133. The slides were mounted using VectaShield media containing the DNA stain DAPI. A single (xy) plane through the colonic crypt structure is shown. Image was obtained using a ×40 oil objective. Pretreatment of the crypts with a MEK-1 inhibitor (PD 98059, 25 μM) and a PKA inhibitor (H89, 10 μM) blocked the 5-min E2-induced phosphorylation of CREB. *Red* shows the nuclei staining, and *green* shows the phospho-CREB staining. The merged *yellow* images indicate that CREB phosphorylated in the vicinity of the DNA. CTL, Control; E2, E2 for 2 min; VEH, vehicle. Each treatment was examined in three rats with five to seven crypts for each treatment per rat. *Scale bar*, 20 μm.

PKCδ in the rat ovary where PKCδ increased during pregnancy and also fluctuated at different stages of luteal differentiation (30). A previous study in uterine tissue demonstrated that PKB was regulated by the sex steroid hormones, and expression fluctuated throughout the reproductive cycle (31). Here we show both PKCδ and PKACI expression levels varied throughout the estrous cycle. PKCδ and PKACI are the major signaling components recruited by estrogen in the antisecretory response. The increased expression of PKCδ and PKACI from proestrus toward the diestrus stage was associated with increased potency of the estrogen inhibition of Cl^- secretion at diestrus. PKCδ and PKACI expression was significantly reduced in proestrus and correlated with minimal inhibition of Cl^- secretion by estrogen. This is the first report of estrous cycle-dependent regulation of protein kinase expression in colonic tissue. It appears that the expression level of the kinases is the rate-limiting factor in determining the potency of the antisecretory response to estrogen.

The rapid estrogen activation of PKA by PKCδ and subsequent association of PKA with the KCNQ1 channel has been shown to be PKCδ dependent in colonic crypts (15). PKA activation appears to be the final step in the inhibition of KCNQ1 channel activity. Indeed, PKA has previously been shown to directly interact with and phosphorylate the channel at Ser27 (32), further indicating it is the last step in the signaling cascade that impacts on the channel. We therefore investigated PKA activation as the endpoint of the rapid antisecretory pathway and whether this activation was also dependent on the stage of the estrous cycle. The results indicated that the timing and intensity of PKA activation by estrogen is dependent on the estrous cycle stage. The failure of estrogen to produce PKA activation at proestrus correlated with minimal inhibition of secretion. Conversely, the maximal PKA activation at diestrus correlated with maximal inhibition of secretion. We hypothesize that the lack of kinase activation by estrogen at proestrus may be due to reduced basal expression levels of PKCδ and PKA. It has previously been determined that the lack of estrogen effects on Cl^- secretion in the male colonic mucosa is due to the low expression of PKCδ compared with the high level in the female tissue (15). PKA activity has been shown to be regulated by the reproductive cycle in the hypothalamus (33). The largest cAMP-induced PKA activation in the hypothalamus was observed during diestrus, similar to the sustained diestrus activation demonstrated in this study. A recent study showed that estrogen-induced acceleration of the oviductal transport of the oocytes in cycling rats was dependent on a successive activation of nongenomic PKA signaling pathways (34). The latter study and the estrous cycle data presented in this paper demonstrate a physiological role for rapid nongenomic PKA activation. The potential for estrogen to inhibit intestinal Cl^- secretion is dependent on a combined effect of enhanced PKCδ and PKA expression and rapid activation of the kinases.

The differences in kinase expression during the estrous cycle indicate the levels are regulated at a genomic level by the sex steroid hormones. It was hypothesized that in addition to causing the rapid antisecretory response by inhibiting KCNQ1 channels, estrogen may also induce a rapid tran-

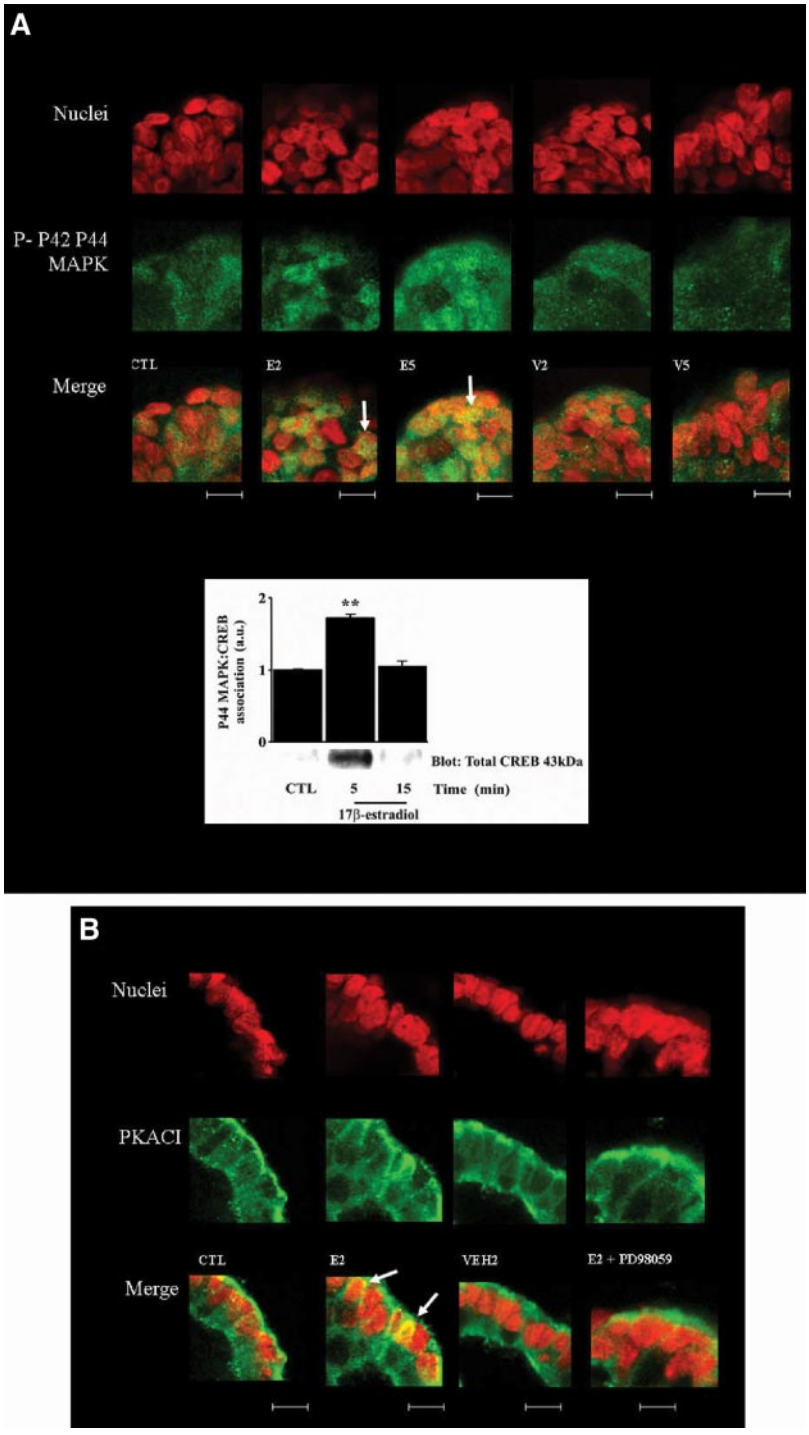

FIG. 7. MAPK and PKA nuclear localization to the nucleus in response to 10 nM E2. A, Isolated colonic crypts were adhered to glass slides, treated as required, and fixed in 4% paraformaldehyde followed by permeabilization in 0.2% Triton X-100 in 1× PBS. The slides were mounted using VectaShield media containing the DNA stain DAPI. Images were obtained using an X63 oil objective through a single (xy) plane. Phospho-P42 P44 MAPK was stained using an antibody to Thr202/Tyr204. *Red* shows the nuclei staining, and *green* shows the phospho-P42/P44 (P-P42 P44) MAPK staining. The merged *yellow* images indicate that MAPK was phosphorylated in the nucleus. The P44 MAPK protein was immunoprecipitated. Western blot analysis was used to detect CREB association after E2 treatment. A representative blot is shown. The *bar graph* shows fold differences over control (n = 3). B, PKA was detected using an antibody to total PKA. *Red* indicates DAPI, and *green* indicates PKA. Merged *yellow* demonstrates perinuclear localization of PKA. CTL, Control; E2, E2 for 2 min; E5, E2 for 5 min; VEH2 (V2), vehicle for 2 min; V5, vehicle for 5 min. Values in the graph are given as fold changes in CREB and MAPK association for colonic crypt samples. Values are displayed as mean ± SEM (n = 3). **, $P < 0.01$. Confocal images for each were obtained from three rats with five to seven crypts for each treatment per rat. *Scale bar*, 5 μm.

scriptional pathway to induce expression of the kinases required to drive the antisecretory response throughout the reproductive cycle. Cross talk between rapid nongenomic and genomic actions of steroid hormones in epithelia is still a mystery. Estrogen may rapidly induce alterations in gene transcription as a result of the activation of second messengers, rather than binding to the classical receptor, and in turn modulate certain transcription factors. We investigated whether the expression of the CREB transcription factor was regulated throughout the estrous cycle. Previous work has demonstrated a reproductive cycle dependence of CREB expression in human endometrium (35) and in rat hypothalamic tissue (36). We hypothesized that regulation of protein kinase expression by estradiol throughout the estrous cycle primes the rapid nongenomic antisecretory action of estrogen. Conversely, the rapid protein kinase activation responses to estrogen also prime the genomic transcriptional pathway. In this way, estradiol works in a bidirectional manner throughout the reproductive cycle. The expression of CREB was shown to be sex specific with approximately eight times more of the protein expressed in the female tissue in comparison with the male. Expression of CREB was also shown to be regulated throughout the estrous cycle. Expression of CREB was low to absent at proestrus followed by a dramatic increase during estrus and a maximal expression at the metestrus stage. The estrous cycle modulation of the regulation of CREB indicates that the rapid phase of estrogen action in the distal colon also regulates transcription. Estrogen induced the phosphorylation of CREB and induction of the expression of CREB itself, PKCδ, and PKA via a rapid MAPK-PKA signaling pathway. P42 P44 MAPK is an important regulator of transcription in epithelial cells. Rapid sex-specific P42 P44 MAPK activation in response to

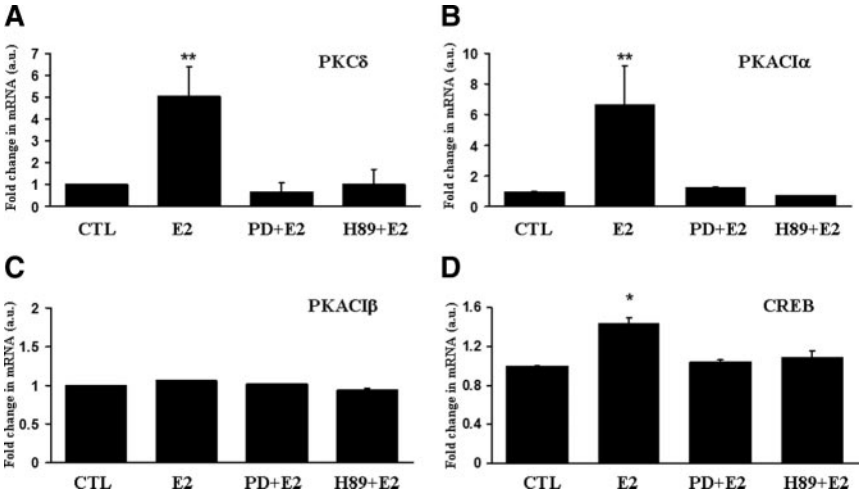

FIG. 8. PKCδ, PKA, and CREB transcription is regulated by E2 in female rat colonic crypts via a PKA/MAPK-dependent pathway. Colonic crypts from male and female rats were treated with E2 (10 nM) for 45 min. Total mRNA was extracted and converted into cDNA. PKCδ (A), PKACIα (B), PKACIβ (C), CREB (D), and β-actin cDNA was analyzed by qRT-PCR using specific primers. E2 up-regulated the mRNA of PKCδ, PKACIα, and CREB. This up-regulation was blocked by pretreatment with the MEK-1 inhibitor PD 98059 (25 μM) and the PKA inhibitor H89 (10 μM). No change was noted for PKACIβ mRNA levels. Values on the graphs are given as mean fold increase compared with control samples. CTL, Control; E, E2; PD + E, PD 98059 plus E2. Values are displayed as mean ± SE (n = 4). *, $P < 0.05$; **, $P < 0.01$, between control and treated values. au, Arbitrary units.

E2 has previously been demonstrated in female growth plate chondrocytes (37). PKC is a known regulator of cellular transcription, and PKCδ has been demonstrated to induce transcription in bronchial epithelial cells via a P42 P44 MAPK pathway (38). A more recent study in uterine tissue demonstrated rapid E2 activation of P42 P44 MAPK via a PKCδ-dependent pathway (39). Thus, a positive feed-forward mechanism for CREB, PKCδ, and PKA expression is driven by rapid E2 activation of PKCδ. This is further evidence for dependence of a genomic response on the rapid induction of kinase activity. P44 MAPK appears to be the signaling protein linking the rapid nongenomic pathway to the genomic pathway. In this study, MAPK is clearly seen to enter and pool within the nucleus. PKA is also responsible for phosphorylating CREB. PKA localizes just inside the nuclear envelope (as seen with merged image of PKA and DAPI signal), and it may phosphorylate CREB within this region. Rapid CREB phosphorylation at Ser133 in response to estrogen has previously been demonstrated to occur via both PKA and MAPK concurrently. A previous study in testicular tissue demonstrated rapid CREB phosphorylation via the membrane ERα, leading to both P42 P44 MAPK and PKA activation, which in turn both modulate the phosphorylation of CREB (blocked by PD 98059 and H89) (26). Another study demonstrated cooperative effects between PKA and MAPK in the phosphorylation of CREB at Ser133 in the nucleus similar to this study (25).

The distal colon was previously thought not to be a target of estrogen until the confirmation of ER expression (40). Increasing evidence suggests that E2 acts via a membrane-bound ER in many cell types (41–44). We have provided evidence for membrane-bound ERα involvement in transducing rapid E2 phosphorylation of PKCδ. The expression of 66-kDa ERα was low in male colonic tissue in comparison with female. We hypothesize that a membrane-bound 66-kDa ERα is the nongenomic receptor transducing the rapid antisecretory actions of E2 in the female distal colon. This is the first report of a gender difference in the expression of the membrane 66-kDa ERα protein. Plasma membrane preparations demonstrated that ERα is present at the plasma membrane to the basolateral side of the cell (with an absence of the truncated 46-kDa ER form) and showed a higher abundance in the female in comparison with the male. Based on this observation, it appears that a membrane-bound 66-kDa ERα is the nongenomic receptor transducing the rapid actions of E2 in the female distal colon.

The fact that the reproductive cycle regulates interrelated nongenomic and genomic actions in the intestine further strengthens the case for a physiological impact of rapid responses to sex steroid hormones. The results presented in this study clearly demonstrated the impact of the reproductive cycle on the intestinal function in the female both at a molecular level through the regulation of protein expression and at a physiological level through the inhibition of transepithelial Cl^- secretion. This is the first report of the modulation of rapid responses to steroid hormones throughout the estrous cycle in the gastrointestinal tract. A previous report demonstrated that estrous cycle differences in dopamine release from rat striatum were primed by differential regulation of the level of cross talk between acute and long-term effects of estrogen through each phase of the cycle (45). In our study, the rapid antisecretory action of E2 was primed throughout the estrous cycle. In addition to the impact of sexual dimorphism on the rapid responses to steroid hormones, the work reported in this paper has demonstrated the reproductive cycle as a new physiological regulatory element in the rapid responses to estrogen. The study also provides novel insights into the molecular and cellular basis for fluid retention in the female in high-estrogen states (Fig. 10).

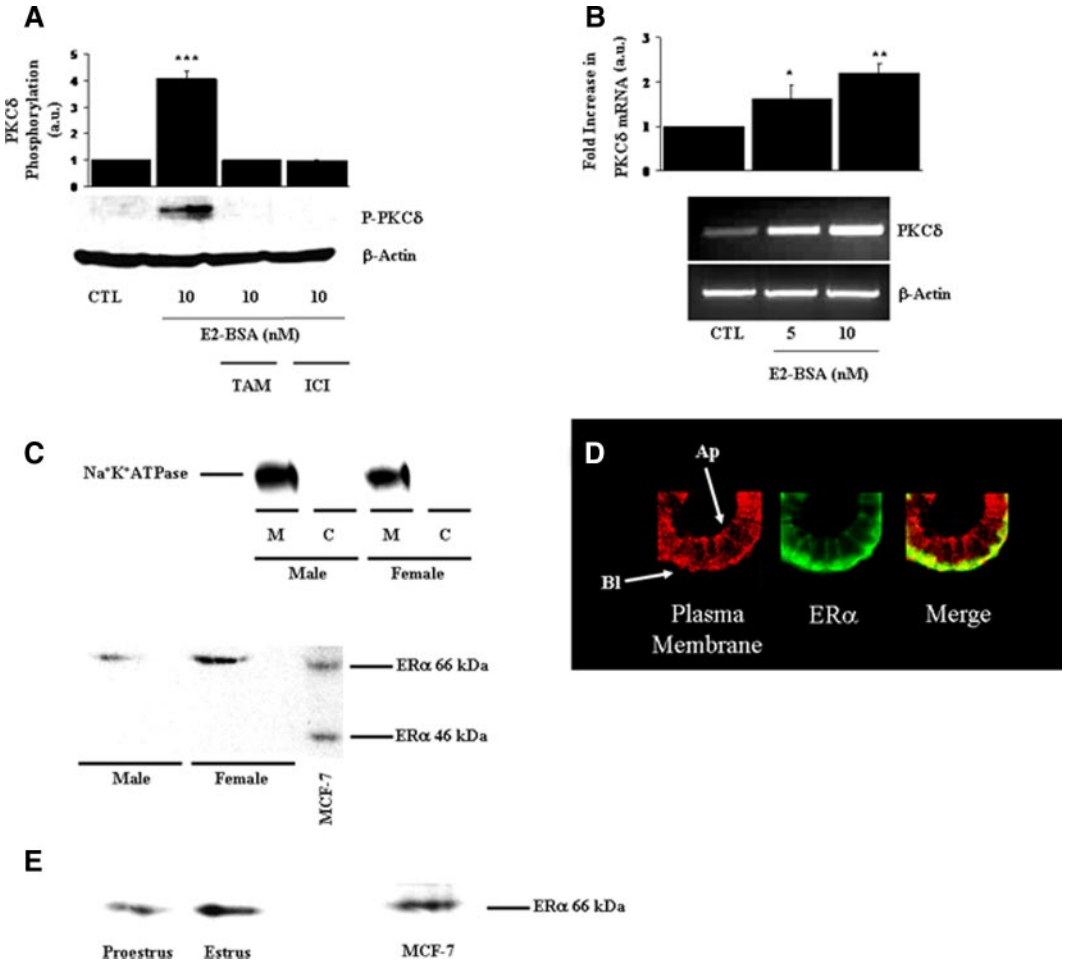

FIG. 9. Estrogen induces signaling and transcriptional responses in the female rat distal colonic crypt via a membrane-bound full-length ERα. A, Colonic crypts from female rats at the estrus stage were treated with charcoal-stripped E2-BSA (10 nM) for 5 min. PKCδ phosphorylation was detected by Western blot analysis and a phospho-PKCδ-specific antibody to Ser643. The increase in E2-BSA-induced PKCδ phosphorylation was blocked by pretreatment with the ERα antagonists ICI 182,780 (1 μM) and tamoxifen (10 μM). B, Colonic crypts from female rats were treated with charcoal-stripped E2-BSA for 45 min. Total mRNA was extracted and converted into cDNA. PKCδ and β-actin cDNA was amplified by PCR using specific primers. E2-BSA (5 and 10 nM) up-regulated PKCδ mRNA. C, Plasma membrane extracts from male and female rat distal colonic crypts were subjected to Western blot analysis, and total ERα was detected. A whole-cell MCF-7 lysate was used as a comparison for ERα sizes. Plasma membrane quality was determined by blotting for Na^+K^+ ATPase. C, Cytosol; M, membrane. D, ERα is associated with the basolateral plasma membrane. Isolated colonic crypts were adhered to glass slides, treated as required, and fixed in 4% paraformaldehyde followed by permeabilization in 0.2% Triton X-100 in 1× PBS. ERα was detected using an antibody to the total protein. The plasma membrane was stained using WGA (1 μg/ml). The slides were mounted using VectaShield media. A single (xy) plane through the colonic crypt structure is shown. The plasma membrane staining is shown in *red*, and the the ERα staining shown in *green*. The merged *yellow* images indicate the association of ERα with the plasma membrane. *Scale bar*, 10 μm. D, Whole-cell lysate from female proestrus and estrus distal colon samples comparing expression of 66-kDa ERα. The figure shows representative Western blots, agarose gels, and confocal images. Values on the graphs are given as a mean fold increase compared with control samples. Ap, Apical; Bl, basolateral; CTL, Control; ICI, ICI 182,780; Tam, tamoxifen. Values are displayed as mean ± SE (A, C, D, and E, n = 3; B, n = 2). ***, $P < 0.001$, between control and treated values.

Materials and Methods

Materials

Total PKCδ and total PKA catalytic subunit isoform I (PKACI) antibodies from BD Transduction (Dorchester, UK). Total CREB, phospho-CREB, total P42 P44 MAPK, and phospho-P42 P44 MAPK were obtained from Cell Signaling Technologies (Beverly, MA). Total ERα antibody was from Santa Cruz Biotechnology (Santa Cruz, CA). Total Na^+K^+ ATPase was obtained from Abcam (Cambridge, UK). Antirabbit and antimouse horseradish peroxidase-linked secondary antibodies were from Sigma-Aldrich (Dublin, Ireland). Goat antirabbit and goat antimouse conjugated to an Alexa 488-nm probe were obtained from Invitrogen (Carlsbad, CA). VectaShield mounting media with a DAPI nuclear stain was from Molecular Probes (Eugene, OR). Plasma membrane staining was obtained using WGA conjugated to Alexa 633 nm. The ECL plus chemiluminescent detection system was from Amersham Biosciences (Little Chalfont, UK) and Bradford reagent from Bio-Rad (Hemel Hempstead, UK). Chromanol 293B, ICI 182,780, and tamoxifen citrate were obtained from Tocris (Bristol, UK). Rottlerin, PD 98059, and H89 were from Calbiochem (Nottingham, UK). All other reagents were obtained from Sigma-Aldrich (Dublin, Ireland) or as stated in the text. E2-BSA was obtained from Steraloids (Newport, RI).

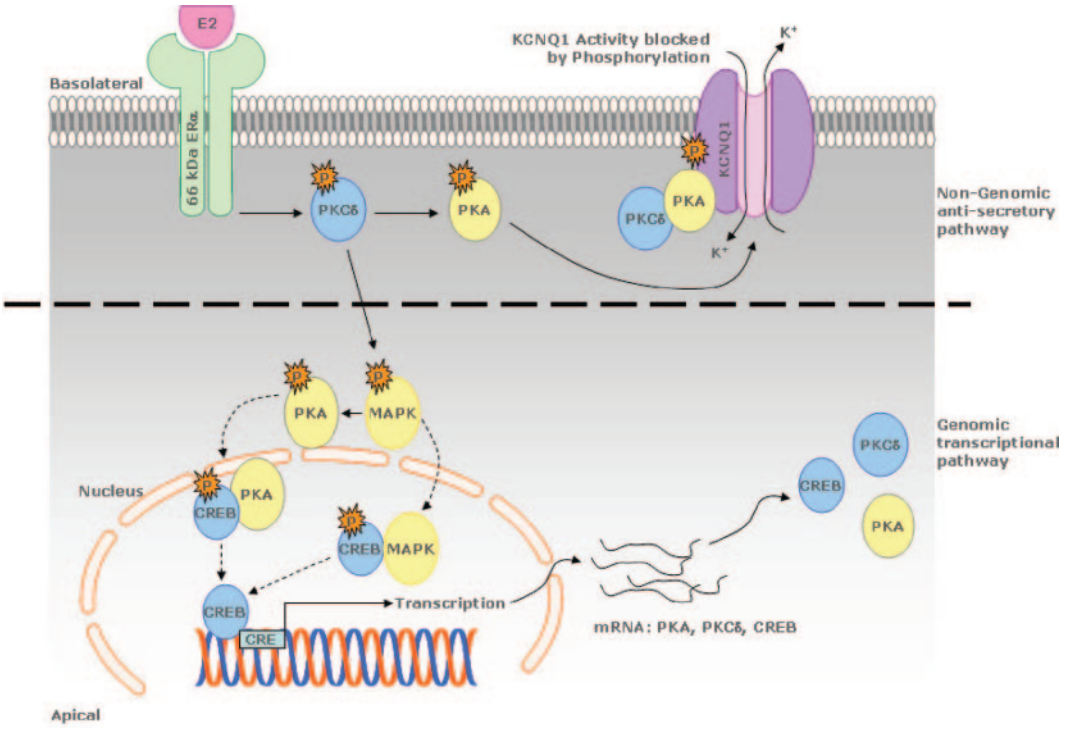

FIG. 10. Proposed model for signal transduction pathways activated by estrogen action in female distal colonic crypts. E2 stimulates PKCδ through a membrane ERα (66-kDa form). PKCδ activates both rapid nongenomic and genomic pathways. PKCδ triggers rapid phosphorylation of PKA, and both kinases translocate to the C terminus of the KCNQ1 channel. Phosphorylation (P) of KCNQ1 Ser27 by PKA blocks channel activity and in turn K^+ recycling, ultimately decreasing the potential for Cl^- secretion. In addition to inducing rapid antisecretory effects, estrogen-activated PKCδ stimulates P44 MAPK. P44 MAPK recruits PKA and translocates to the nucleus, whereupon PKA enters the cell but remains close to the edge of the nucleus. MAPK enters and is seen to be throughout the nucleus. Both kinases phosphorylate the transcription factor CREB. PKA and MAPK both phosphorylate CREB. Dual regulation of CREB by both kinases has previously been documented in other systems (25, 26).

Animals

Both male (~350 g) and female (~300 g) Sprague Dawley rats from 8–12 wk old were used for all experiments. The females become sexually mature at about 35 wk, allowing for determination of the estrous cycle (46). Circulating E2 levels in the rat increase during proestrus and subsequently impact on the following estrus stage followed by a decrease throughout metestrus and diestrus (47, 48). The animals were maintained on a 12-h light, 12-h dark cycle and were given *ad libitum* access to food and water. Anesthetized rats were killed by cervical dislocation. Cervical smears were obtained from female rats by flushing the vaginal canal with Krebs solution, and the stage of the estrous cycle was determined histologically as previously described (49).

The distal colon was removed to below the pelvic rim. The fecal contents were rinsed, and distal colonic crypts were isolated as previously described (50). Isolations and treatments were carried out at room temperature to avoid colonic crypt disintegration (50, 51). Sheets of colonic mucosa were obtained by blunt dissection for transepithelial transport measurements. All procedures were approved by the Royal College of Surgeons in Ireland Ethics Committee.

Transepithelial transport studies

Colonic epithelia was stripped from the muscle tissue and placed on inserts exposing an area of 0.5 cm^2. The inserts were mounted in Ussing chambers (Physiologic Instruments, San Diego, CA). Transepithelial potential difference was clamped to 0 mV using an EVC-4000 voltage-clamp apparatus (World Precision Instruments, Stevenage, UK). Transepithelial short-circuit current (I_{SC}) was recorded using Ag-AgCl electrodes in 3 M KCl agar bridges. Both apical and basolateral baths were filled with Krebs bicarbonate buffer (in mM): 120 NaCl, 25 $NaHCO_3$, 3.3 KH_2PO_4, 0.8 K_2HPO_4, 1.2 $MgCl_2$, 1.2 $CaCl_2$, 10 glucose (pH 7.4). The chambers were maintained at 37 C by heated water jackets and oxygenated with a 95% O_2/5% CO_2 mixture. The colonic tissue preparations were allowed to equilibrate for 30–45 min before commencing treatments. The I_{SC} was defined as positive for anion flow from the basolateral to apical chamber and for cation flow in the opposite direction.

Immunoprecipitation and Western blotting

After isolation, the distal colonic crypts were resuspended in Krebs solution. The crypts were treated with the appropriate drug for the indicated time points. After treatment, the samples were lysed as previously described (15). Immunoprecipitations were carried out as previously described (15). The protein content of the supernatant was quantified by the Bradford method (52). For all activation assays, 50 μg sample was combined with 2× Laemmli buffer, boiled at 95 C for 5 min, and spun at 12,000 rpm for 2 min. Western blot analysis was carried out as standard. Protein was transferred to polyvinylidene difluoride membranes, blocked in 1× Tris-buffered saline with 1% Tween 20 and 5% nonfat dry milk for 1 h. Membranes were incubated with the appropriate primary antibody overnight at 4 C and incubated for 1 h at room temperature with the appropriate secondary antibody. Membranes were washed in 1× Tris-

buffered saline with 1% Tween 20 three times for 15 min. Bands were detected using autoradiographic film and chemiluminescence. The membranes were stripped using a high-salt stripping buffer (Promega, Southampton, UK) to obtain loading levels of β-actin.

PKA activation assay

PKA activation was measured using a PepTag Assay for the nonradioactive detection of cAMP-dependent protein kinase (Promega) according to the manufacturer's instructions with minor modifications; 2.5 μl F-Kemptide PepTag and 2.5 μl cAMP activator solution were added instead of 5 μl.

Immunofluorescence and confocal microscopy

Isolated female crypts were adhered to eight-well slides (Nunc, Rochester, NY) using Cell-Tak (BD Biosciences, UK) using the adsorption technique (according to the manufacturer's instructions). Adhered crypts were treated as required and washed with ice-cold 1× PBS to halt the treatment. The cells were fixed in 4% paraformaldehyde solution (dissolved at 70 C in 1× PBS) at room temperature. The crypts were then permeabilized in 0.2% Triton X-100 in 1× PBS. The crypts were rinsed in 1× PBS and incubated at room temperature for 15 min in a 3% BSA blocking buffer to avoid nonspecific binding of antibodies and fluorescent conjugates. After this, the antibody solution (phospho-CREB, 1:100 dilution; phospho-MAPK P42 P44, 1:100 dilution; PKACI, 1:100 dilution; ERα, 1:100 dilution) was added in 2% BSA blocking buffer for 1 h at room temperature. The crypts were washed twice in 0.2% BSA buffer, and the rabbit secondary antibody (Alexa Fluor 488 conjugated) was added in a 2% BSA buffer. The cells were washed three times with a 0.2% BSA solution and twice with 1× PBS. The slides were then mounted in VectaShield (Vector Laboratories, Burlingame, CA) with DAPI DNA stain. Single crypts were imaged using a ×40 oil objective on a Zeiss LSM 510 confocal microscope. Detailed images of colonic crypt nuclei were obtained using a ×63 oil objective. The excitation wavelengths for WGA, Alexa Fluor 488, and DAPI were 633, 488, and 345 nm, respectively.

Total RNA preparation, RT-PCR analysis, and real-time PCR analysis

RNA extracts were prepared from female rat colonic crypts at the estrus stage of the estrous cycle using the QIAGEN RNeasy kit (QIAGEN, Crawley, UK). Because the RNA was from primary tissue, we carried out a genomic DNA treatment as a precaution. Any contaminating genomic DNA was digested using the DNA-*free* kit as per manufacturer's instructions (Ambion, Huntingdon, UK). Single-strand cDNA was synthesized using the Improm II reverse transcriptase system (Promega). The synthesized cDNA was quantified at 260 nm and corrected for loading differences in RT-PCR reaction mixes. PKA isoform I has three catalytic subunits (α, β, and γ) and two regulatory subunits (α and β). PKACIγ and PKARIβ were not examined because these subunit isotypes are primarily expressed in nervous and adipose tissues. PKCδ (NM_133307; forward, 5′-caccatcttccagaaagaacg-3′; reverse, 5′-cttgccatag-gtcccgttgttg-3′; product size, 352 bp), PKACIα (X57986; forward, 5′-tcctttgggcgagtgatgc-3′; reverse, 5′-gcgaagaagggcggg-taac-3′; product size, 563 bp), PKACIβ (D10770; forward, 5′-cagatcgtgctaacatttgag-3′; reverse, 5′-gtcatcgaagttgctggtatc-3′; product size, 543 bp), PKARIα (NM_013181; forward, 5′-gcaagacagattcagagcc-3′; reverse, 5′-ggttgcccattcattattg-3′; product size,393 bp), and CREB (NM_134443; forward, 5′-agcccctgccatcaccact-3′; reverse, 5′-tgctgcttccctgttcttcattag-3′; product size, 409 bp) primers were designed using primer 3 analysis (http://frodo.wi.mit.edu/primer3/). GoTaq polymerase mix from Promega was used in the amplification. Touchdown PCR was used to amplify the cDNA for 25 cycles over an annealing temperature range of 59–49 C in the case of PKACIα, PKACIβ, PKARIα, and CREB. PKCδ was amplified over a range of 65–55 C for 25 cycles. β-Actin (NM_031144; forward, 5′-cagtaatctccttctgcatcc-3′; reverse, 5′-actacctcatgaagatcctga-3′; product size, 350 bp) was amplified for 25 cycles at an annealing temperature of 52 C. Amplicons were analyzed on a 2% 1× Tris-acetate-EDTA agarose gel and imaged using a UV light source. A 100-bp marker was employed to determine whether the amplicons were the correct size. PCR analysis was carried out using the RNA preparations as the template to ensure an absence of interfering genomic DNA. Real-time PCR analysis was carried out using the Bio-Rad iCycler and SYBR GreenER qPCR SuperMix (Invitrogen) according to manufacturer's instructions. The PCR program was set up as described in the SuperMix protocol (Invitrogen). A melting-curve analysis was performed for all primer sets after PCR analysis to ensure the absence of nonspecific amplicons and also primer-dimers. A change in transcript levels was determined by the $\Delta\Delta C_t$ method. β-Actin was used as an internal control.

Plasma membrane extraction

Plasma membrane was extracted using the Mem-PER eukaryotic membrane protein extraction kit from Promega. The plasma membrane was extracted according to the kit's instructions. The quality of extract was compared between cytosolic fraction and membrane fraction by immunoblotting for the plasma membrane marker Na^+K^+ ATPase.

Statistical and densitometric analysis

For the study, the data are presented as mean ± SEM for a series of the indicated number of experiments. Statistical analysis of the data was obtained by analysis using one-way ANOVA and Tukeys *post hoc* test for multiple analysis of more than two groups. Densitometric analysis of Western blots, PKA assays, and RT-PCR images were performed using GeneTools software (Syngene, Cambridge, UK).

Acknowledgments

Address all correspondence and requests for reprints to: Fiona O'Mahony, Ph.D., Department of Molecular Medicine, Royal College of Surgeons in Ireland, Education and Research Centre Smurfit Building, Beaumont Hospital, P.O. Box 9063, Dublin 9, Ireland. E-mail: fomahony@rcsi.ie.

This work was supported by The Wellcome Trust Program Grant 06089/Z/00/Z and Higher Education Authority of Ireland (HEA) PRTLI Grant Cycle 3. R.A. was recipient of a Wellcome Trust Studentship Prize 06379/Z/01/Z. F.O.M. is supported by a postdoctoral fellowship grant from the National Biophotonics and Imaging Platform of Ireland.

Disclosure Summary: The authors have nothing to disclose.

References

1. **Westerholm B** 1980 Clinical toxicology of estrogens. Pharmacol Ther 10:337–349
2. **Weenink GH, Ten Cate JW, Kahle LH, Lamping RJ, Treffers PE** 1981 "Morning after pill" and antithrombin III. Lancet 1:1105
3. **Stachenfeld NS, DiPietro L, Palter SF, Nadel ER** 1998 Estrogen influences osmotic secretion of AVP and body water balance in postmenopausal women. Am J Physiol 274:R187–R195
4. **Harvey BJ, Condliffe S, Doolan CM** 2001 Sex and salt hormones: rapid effects in epithelia. News Physiol Sci 16:174–177
5. **Johnson JA, Davis JO** 1976 The effect of estrogens on renal sodium excretion in the dog. Perspect Nephrol Hypertens 5:239–248
6. **Sweezey N, Tchepichev S, Gagnon S, Fertuck K, O'Brodovich H** 1998 Female gender hormones regulate mRNA levels and function of the rat lung epithelial Na channel. Am J Physiol 274:C379–C386
7. **Condliffe SB, Doolan CM, Harvey BJ** 2001 17β-Oestradiol acutely regulates Cl^- secretion in rat distal colonic epithelium. J Physiol 530:47–54
8. **Jung HK, Kim DY, Moon IH** 2003 Effects of gender and menstrual cycle on colonic transit time in healthy subjects. Korean J Intern Med 18:181–186
9. **Córdova-Fraga T, Huerta-Franco R, Gutiérrez-Juárez G, Sosa-Aquino M, Vargas-Luna M** 2004 The colon transit time in different phases of the menstrual cycle: assessed with biomagnetic technique. Neurol Clin Neurophysiol 2004:31
10. **Woods NF, Lentz MJ, Mitchell ES, Shaver J, Heitkemper M** 1998 Luteal phase ovarian steroids, stress arousal, premenses perceived stress, and premenstrual symptoms. Res Nurs Health 21:129–142
11. **Christofferson RH, Nilsson BO** 1988 Morphology of the endometrial microvasculature during early placentation in the rat. Cell Tissue Res 253:209–220
12. **Halm ST, Liao T, Halm DR** 2006 Distinct K^+ conductive pathways are required for Cl^- and K^+ secretion across distal colonic epithelium. Am J Physiol Cell Physiol 291:C636–C648
13. **Kunzelmann K, Hübner M, Schreiber R, Levy-Holzman R, Garty H, Bleich M, Warth R, Slavik M, von Hahn T, Greger R** 2001 Cloning and function of the rat colonic epithelial K^+ channel KV-LQT1. J Membr Biol 179:155–164
14. **McNamara B, Winter DC, Cuffe JE, O'Sullivan GC, Harvey BJ** 1999 Basolateral K^+ channel involvement in forskolin-activated chloride secretion in human colon. J Physiol 519(Pt 1):251–260
15. **O'Mahony F, Alzamora R, Betts V, LaPaix F, Carter D, Irnaten M, Harvey BJ** 2007 Female gender-specific inhibition of KCNQ1 channels and chloride secretion by 17β-estradiol in rat distal colonic crypts. J Biol Chem 282:24563–24573
16. **Johannessen M, Moens U** 2007 Multisite phosphorylation of the cAMP response element-binding protein (CREB) by a diversity of protein kinases. Front Biosci 12:1814–1832
17. **Smith CL, Oñate SA, Tsai MJ, O'Malley BW** 1996 CREB binding protein acts synergistically with steroid receptor coactivator-1 to enhance steroid receptor-dependent transcription. Proc Natl Acad Sci USA 93:8884–8888
18. **Beyer C, Karolczak M** 2000 Estrogenic stimulation of neurite growth in midbrain dopaminergic neurons depends on cAMP/protein kinase A signalling. J Neurosci Res 59:107–116
19. **Roux PP, Blenis J** 2004 ERK and p38 MAPK-activated protein kinases: a family of protein kinases with diverse biological functions. Microbiol Mol Biol Rev 68:320–344
20. **Lenormand P, Pagès G, Sardet C, L'Allemain G, Meloche S, Pouysségur J** 1993 MAP kinases: activation, subcellular localization and role in the control of cell proliferation. Adv Second Messenger Phosphoprotein Res 28:237–244
21. **Lenormand P, Sardet C, Pagès G, L'Allemain G, Brunet A, Pouysségur J** 1993 Growth factors induce nuclear translocation of MAP kinases (p42mapk and p44mapk) but not of their activator MAP kinase kinase (p45mapkk) in fibroblasts. J Cell Biol 122:1079–1088
22. **Gschwendt M, Müller HJ, Kielbassa K, Zang R, Kittstein W, Rincke G, Marks F** 1994 Rottlerin, a novel protein kinase inhibitor. Biochem Biophys Res Commun 199:93–98
23. **Alessi DR, Cuenda A, Cohen P, Dudley DT, Saltiel AR** 1995 PD 098059 is a specific inhibitor of the activation of mitogen-activated protein kinase kinase in vitro and in vivo. J Biol Chem 270:27489–27494
24. **Lochner A, Moolman JA** 2006 The many faces of H89: a review. Cardiovasc Drug Rev 24:261–274
25. **Costes S, Longuet C, Broca C, Faruque O, Hani EH, Bataille D, Dalle S** 2004 Cooperative effects between protein kinase A and p44/p42 mitogen-activated protein kinase to promote cAMP-responsive element binding protein activation after β-cell stimulation by glucose and its alteration due to glucotoxicity. Ann NY Acad Sci 1030:230–242
26. **Bouskine A, Nebout M, Mograbi B, Brücker-Davis F, Roger C, Fenichel P** 2008 Estrogens promote human testicular germ cell cancer through a membrane-mediated activation of extracellular regulated kinase and protein kinase A. Endocrinology 149:565–573
27. **Doolan CM, Condliffe SB, Harvey BJ** 2000 Rapid non-genomic activation of cytosolic cyclic AMP-dependent protein kinase activity and $[Ca^{2+}]_i$ by 17β-oestradiol in female rat distal colon. Br J Pharmacol 129:1375–1386
28. **Winnard KP, Dmitrieva N, Berkley KJ** 2006 Cross-organ interactions between reproductive, gastrointestinal, and urinary tracts: modulation by estrous stage and involvement of the hypogastric nerve. Am J Physiol Regul Integr Comp Physiol 291:R1592–R1601
29. **Houdeau E, Larauche M, Monnerie R, Bueno L, Fioramonti J** 2005 Uterine motor alterations and estrous cycle disturbances associated with colonic inflammation in the rat. Am J Physiol Regul Integr Comp Physiol 288:R630–R637
30. **Cutler Jr RE, Maizels ET, Hunzicker-Dunn M** 1994 Delta protein kinase-C in the rat ovary: estrogen regulation and localization. Endocrinology 135:1669–1678
31. **Dery MC, Leblanc V, Shooner C, Asselin E** 2003 Regulation of Akt expression and phosphorylation by 17β-estradiol in the rat uterus during estrous cycle. Reprod Biol Endocrinol 1:47
32. **Kurokawa J, Motoike HK, Rao J, Kass RS** 2004 Regulatory actions of the A-kinase anchoring protein Yotiao on a heart potassium channel downstream of PKA phosphorylation. Proc Natl Acad Sci USA 101:16374–16378
33. **Ostrowska A** 1994 The activation of protein kinase A by cyclic AMP is influenced by oestradiol and progesterone in supernatants from the anterior pituitary but not from hypothalamus of the female rat. Biol Cell 81:223–226
34. **Orihuela PA, Parada-Bustamante A, Zuñiga LM, Croxatto HB** 2006 Inositol triphosphate participates in an oestradiol non-genomic signalling pathway involved in accelerated oviductal transport in cycling rats. J Endocrinol 188:579–588
35. **Vienonen A, Miettinen S, Bläuer M, Martikainen PM, Tomás E, Heinonen PK, Ylikomi T** 2004 Expression of nuclear receptors and cofactors in human endometrium and myometrium. J Soc Gynecol Investig 11:104–112
36. **Mogi K, Funabashi T, Mitsushima D, Hagiwara H, Kimura F** 2005 Sex difference in the response of melanin-concentrating hormone neurons in the lateral hypothalamic area to glucose, as revealed by the expression of phosphorylated cyclic adenosine 3′,5′-monophosphate response element-binding protein. Endocrinology 146:3325–3333
37. **McMillan J, Fatehi-Sedeh S, Sylvia VL, Bingham V, Zhong M, Boyan BD, Schwartz Z** 2006 Sex-specific regulation of growth plate chondrocytes by estrogen is via multiple MAP kinase signaling pathways. Biochim Biophys Acta 1763:381–392
38. **Vuong H, Patterson T, Shapiro P, Kalvakolanu DV, Wu R, Ma WY, Dong Z, Kleeberger SR, Reddy SP** 2000 Phorbol ester-induced expression of airway squamous cell differentiation marker, SPRR1B, is regulated by protein kinase Cδ/Ras/MEKK1/MKK1-dependent/AP-1 signal transduction pathway. J Biol Chem 275:32250–32259
39. **Shum JK, Melendez JA, Jeffrey JJ** 2002 Serotonin-induced

MMP-13 production is mediated via phospholipase C, protein kinase C, and ERK1/2 in rat uterine smooth muscle cells. J Biol Chem 277:42830–42840
40. **Thomas ML, Xu X, Norfleet AM, Watson CS** 1993 The presence of functional estrogen receptors in intestinal epithelial cells. Endocrinology 132:426–430
41. **Pappas TC, Gametchu B, Watson CS** 1995 Membrane estrogen receptors identified by multiple antibody labeling and impeded-ligand binding. FASEB J 9:404–410
42. **Pietras RJ, Nemere I, Szego CM** 2001 Steroid hormone receptors in target cell membranes. Endocrine 14:417–427
43. **Razandi M, Pedram A, Merchenthaler I, Greene GL, Levin ER** 2004 Plasma membrane estrogen receptors exist and functions as dimers. Mol Endocrinol 18:2854–2865
44. **Yang JZ, O'Flatharta C, Harvey BJ, Thomas W** 2008 Membrane ERα-dependent activation of PKCα in endometrial cancer cells by estradiol. Steroids 73:1110–1122
45. **Becker JB, Rudick CN** 1999 Rapid effects of estrogen or progesterone on the amphetamine-induced increase in striatal dopamine are enhanced by estrogen priming: a microdialysis study. Pharmacol Biochem Behav 64:53–57
46. **Nequin LG, Alvarez J, Schwartz NB** 1979 Measurement of serum steroid and gonadotropin levels and uterine and ovarian variables throughout 4 day and 5 day estrous cycles in the rat. Biol Reprod 20:659–670
47. **Haim S, Shakhar G, Rossene E, Taylor AN, Ben-Eliyahu S** 2003 Serum levels of sex hormones and corticosterone throughout 4- and 5-day estrous cycles in Fischer 344 rats and their simulation in ovariectomized females. J Endocrinol Invest 26:1013–1022
48. **Mannino CA, South SM, Inturrisi CE, Quinones-Jenab V** 2005 Pharmacokinetics and effects of 17β-estradiol and progesterone implants in ovariectomized rats. J Pain 6:809–816
49. **Hubscher CH, Brooks DL, Johnson JR** 2005 A quantitative method for assessing stages of the rat estrous cycle. Biotech Histochem 80:79–87
50. **Doolan CM, Harvey BJ** 1996 Modulation of cytosolic protein kinase C and calcium ion activity by steroid hormones in rat distal colon. J Biol Chem 271:8763–8767
51. **Schultheiss G, Lan Kocks S, Diener M** 2002 Methods for the study of ionic currents and Ca^{2+}-signals in isolated colonic crypts. Biol Proced Online 3:70–78
52. **Bradford MM** 1976 A rapid and sensitive method for the quantitation of microgram quantities of protein using the principle of protein-dye binding. Anal Biochem 72:248–254

NIDDK Workshop on Circadian Rhythms and Metabolic Disease

April 12–13, 2010
Marriott North Bethesda Hotel and Conference Center, Bethesda, MD

This workshop seeks to gain a better understanding of the link between circadian rhythms and human health and disease. Emphasis will be placed on the influence of central and cellular clocks on the physiology of behavior and metabolism, specifically on overall energy balance and obesity. The goal will be to identify areas of future research to better elucidate the contribution of circadian rhythms to metabolism and disease.

Further information may be obtained at http://www3.niddk.nih.gov/fund/other/circadian2010. For additional information contact Ronald Margolis, Ph.D., 301-594-8819/margolisr@mail.nih.gov.